A HIERARCHY OF MODELS FOR MULTILANE VEHICULAR TRAFFIC II: NUMERICAL AND STOCHASTIC INVESTIGATIONS

A. Klar
Fachbereich Mathematik, Universität Kaiserslautern
Kaiserslautern, Germany

R. Wegener
Institut für Techno- und Wirtschaftsmathematik
Kaiserslautern, Germany

January 16, 1998

Abstract

In this paper the work presented in [6] is continued. The present paper contains detailed numerical investigations of the models developed there. A numerical method to treat the kinetic equations obtained in [6] are presented and results of the simulations are shown. Moreover, the stochastic correlation model used in [6] is described and investigated in more detail.

1 Introduction

In this part we present numerical methods and results for the equations of vehicular traffic, which have been obtained in [6]. We refer to [6] as Part I. The microscopic, the kinetic and the macroscopic model are considered and detailed numerical results are given.

The paper is organized in the following way: In Section 2 we describe results obtained with the microscopic model described in I, Section 2. We evaluate explicitely the velocity distribution functions, the fundamental diagram, and the leading vehicle distribution from the microscopic model. Section 3 contains the description of the method to simulate the homogeneous kinetic model and describes the way, the coefficients of the macroscopic model are determined numerically. To obtain these coefficients one uses the stationary distributions of the homogenous cumulative kinetic equation as described in I. The results of microscopic and kinetic simulations

are compared. Section 4 describes inhomogeneous situations. The macroscopic equations with the above mentioned coefficients are solved and results for a highway with a reduction of lanes are shown. In Section 5 a stochastic model is included, which is used in I, section 3 to obtain several quantities needed to set up the kinetic model, like the correlation function and the lane changing probabilities. This stochastic model is defined and investigated in more detail.

The physical units in the following numerical computations are fixed by setting the maximal velocity w equal to 1 and the bumper to bumper distance H_0 equal to 1. Thus, the maximal density per lane is $\rho_m = \frac{1}{H_0} = 1$ and the unit time t_0 is given by $t_0 = \frac{H_0}{w} = 1$.

2 Simulation of the Microscopic Model

The microscopic model defined in I, Section 2 is considered for an equilibrium situation. We consider a periodic highway with length L. The highway has N lanes and a total density $N\rho$, where ρ denotes the average density per lane. ρ is given by $\rho = \frac{M}{L}$ where NM denotes the total number of cars on the highway.

The simulation is based on an event oriented scheme, i.e. the exact trajectory of any single vehicle is calculated from one event (interaction) to the next. During the interaction the velocities are changed according to the rules set up in I, Section 2.

In the actual computation the length of the highway under consideration is chosen as $L = 500$. The number of lanes is choosen as $N = 3$. For the reaction times the following values have been used: $T_B = 5, T_A = 10, T_F = 20, T_L \sim T_B \sim T_R, T_L^S = T_B = T_R^S$. Moreover, we choose $\alpha = 2, \beta = 0.5, \delta = 0.1$ and $f_D = \frac{1}{0.05}\chi_{[0.95,1]}$. We refer to [4] for experimental data.

The number of vehicles is then defined by the desired value of ρ. Starting with an uniform distribution in space, a random distribution in velocity is chosen such that the distance between vehicle i and its leading car is at least the braking distance $H_B(v_i)$, where v_i is the velocity of vehicle i, $i = 1, \cdots, NM$. The evolution is computed until a stationary state is reached. We use a large number of iterations and time averaging at the end of these iterations.

In Figure (1) the time development of the mean velocity $\frac{1}{NM}\sum_{i=1}^{NM} v_i$, computed with the microscopic model for situations with densities $\rho = 0.1, 0.2, 0.4, 0.6$, is shown. One observes a fast tendency towards equilibrium with fluctuations around the equilibrium state. The fluctuations depend on the number of vehicles. We mention that other quantities like higher order moments need a longer time to reach the final equilibrium state. The numerical simulations support the assumption that the equilibrium state is determined by one parameter, the density ρ.

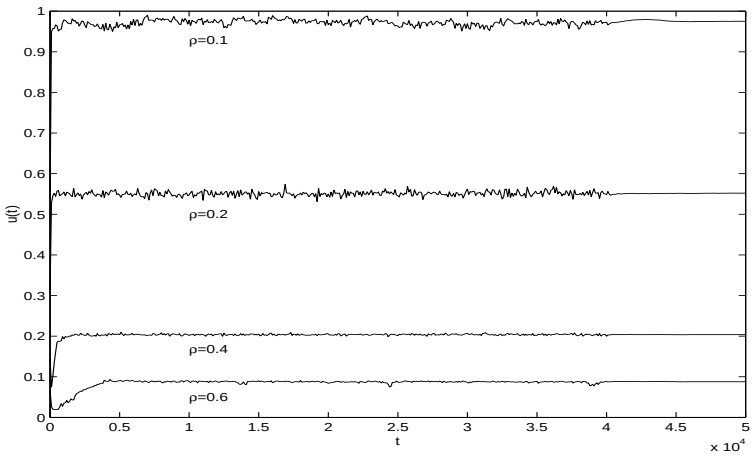

Figure 1: Approach to the stationary state of the mean velocity for $\rho = 0.1, 0.2, 0.4.0.6$ (averaging for $t > 4 \cdot 10^4$)

In Figure (2) we plot the velocity distribution functions for different values of ρ. The plot shows the distribution of the velocities after the final stationary state has been reached. The kinetic distribution functions for the same values of ρ are plotted in Figure (4).

The mean velocities for the whole range of values of ρ, associated to these distribution functions, i.e. the fundamental diagram, is shown in Figure (3). It is plotted together with the kinetic fundamental diagram $u^e(\rho)$ defined in I, Section 4.2, (17), obtained from the stationary distributions of the homogeneous kinetic equation.

In Figure (9) we show the distribution of the distances of the leading vehicles obtained from the stationary state of the microscopic model for $\rho = 0.4$. It is compared with the velocity averaged kinetic distribution of the leading vehicles. This distribution is obtained by using assumption (2), see also (6) in I, Section 3.1, combined with the stationary solution of the homogeneous kinetic equation.

If, e.g., the fundamental diagram is compared with measured data, as reported in [7], one observes good qualitative agreement.

Moreover, one observes, as will be discussed in more detail in the next section, good agreement of the microscopic with the kinetic results. This gives a numerical justification for the derivation procedure leading to the kinetic equation presented in Part I.

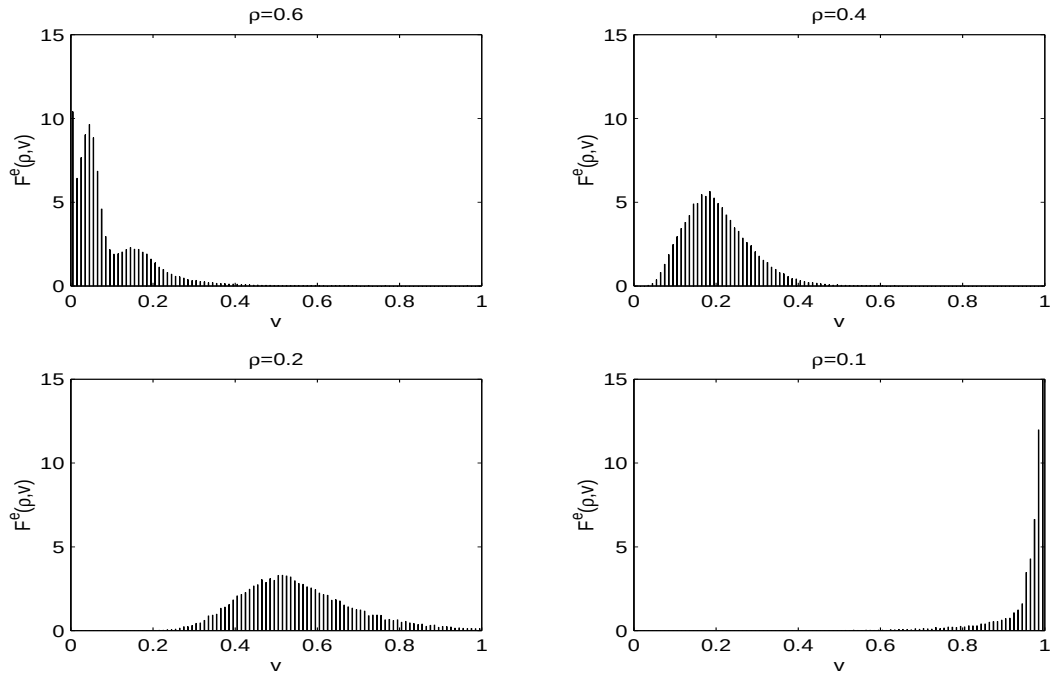

Figure 2: Distribution function for $\rho = 0.1, 0.2, 0.4.0.6$

3 Simulation of the Homogeneous Kinetic Model and Macroscopic Coefficients

To obtain the coefficients for the fluid dynamic equations we have to compute the stationary distributions of the homogeneous cumulative kinetic equation I, (16). We treat the kinetic equation by a discretization scheme, that is described in the following:

A simple standard discretization of the equation in velocity-space needs a large number of discretization points in order to describe correctly the influence of the singularities appearing at $v = 0$ and $v = w = 1$. Therefore, we divide the velocity space into a certain number of cells and calculate the transition rates between the cells given by the kinetic equation. One uses either a fixed or an adaptive grid in velocity space. To get accurate solutions the use of an adaptive grid, concentrating the grid points around the peaks of the distribution function, gives a big advantage in computation time. Here we describe for simplicity the procedure with a fixed discretization. We introduce gridpoints

$$v_i = \frac{i}{K-1}, \quad i = 0, \ldots, K-1$$

in $[0, 1]$. Integrating the distribution function f over each cell M_i with $M_0 =$

$[0, \frac{1}{2(K-1)}]$, $M_i = [\frac{i-\frac{1}{2}}{K-1}, \frac{i+\frac{1}{2}}{K-1}], i = 1, \cdots K-2$ and $M_{K-1} = [1 - \frac{1}{2(K-1)}, 1]$, gives

$$h_i = \int_{M_i} f(v)dv.$$

The discretized kinetic equation is then given by integrating the kinetic equation I, (16) with respect to v over each cell M_i. This gives

$$\partial_t h_i = \int_{M_i} C_C(f)(v)dv.$$

Using the integration rule

$$\int_0^w \psi(v)f(v)dv \sim \sum_{i=0}^{K-1} \psi(v_i)h_i$$

one obtains a discrete velocity model:

$$\partial_t h_i = \sum_{j,k=0}^{K-1} S_{ijk}h_j h_k.$$

The transition rates S_{ijk} are determined by an explicit integration of the collision kernels over the cells M_i. The most important fact about this type of discretization is the conservation of density (number of vehicles). One shows

$$\sum_{i=0}^{K-1} S_{ijk} = 0.$$

This gives the assertion due to $\rho = \sum_{j=0}^{K-1} h_i$.

In the following simulations of the kinetic model the same parameters for the reaction times as in the microscopic model are used.

Figure (3) shows plots of the kinetic fundamental diagrams $u^e(\rho)$. This means we plot the mean values of the stationary distributions of the homogeneous kinetic equation I, (16) for the whole range of values of ρ. For the numerical simulation the parameter λ in the definition I, (6) of the leading vehicle distribution q has been choosen equal to 0 and $1 - \epsilon$, where ϵ is small. (λ did denote the part of the vehicles having a following behaviour, see also Section 5.1.). We remark that the results are not sensitive to the exact choice of ϵ. Moreover, the microscopic fundamental diagram is plotted. The plot of the mean velocity obtained from the kinetic model with $\lambda = 1 - \epsilon$ agrees very well with the microscopic fundamental diagram. This shows that in our microscopic simulation essentially all cars have a following behaviour. In particular, for densities larger than $\rho = 0.15$ the agreement is very good. This corresponds to the fact that for higher densities all cars are trapped between braking and acceleration line. This behaviour is generally not true

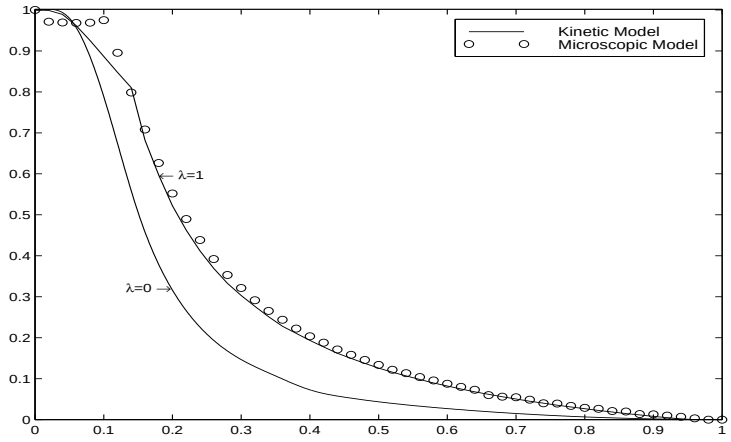

Figure 3: Kinetic ($\lambda = 0, 1 - \epsilon$) and microscopic fundamental diagrams

in practice for small values of ρ. Independent cars appear as well. Another choice of λ could be more appropriate in these situations. We mention, that measured data for the fundamental diagram are reported, e.g., in [7]. As mentioned above the qualitative agreement with these data is good.

In order to obtain a good agreement of microscopic and kinetic results and for reasons of simplicity, we have choosen in the following $\lambda = 1 - \epsilon$. Figure (4) shows the stationary distributions $f^e(\rho)$ of the homogeneous kinetic equation for different values of ρ. This may be compared to the microscopic distribution functions shown in Figure (2). One observes a good aggreement for most of the values of ρ. However, for ρ very small or very large the form of the microscopic and kinetic distribution functions deviates. This is, for example, due to the additional accelerations in the microscopic model.

In the following all quantities defined in I, Section 4.2 are determined. Figure (5) shows a plot of the traffic pressure $p_e(\rho)$. The Enskog coefficient $A^e(\rho)$ is shown in Figure (6). We mention that the values of the Enskog coefficient are much larger than those of $p_e(\rho)$. Figure (7) shows a plot of the lane changing probabilities $P_Y^e(\rho) = P_R^e(\rho) = P_L^e(\rho)$. Equality is due to the fact that we have choosen $T_L^S = T_R^S$. Figure (7) shows the lane changing probabilities due to interactions. In general, also spontaneous lane changing has to be taken into account, which is not caused by another car. This type of lane changing has for simplicity not been considered in the model up to now, see also Remark 3 in I, Section 2. However, in particular, for inhomogeneous situations like the one treated in the next section, it is important to include this kind of lane changing. Figure (8) shows a plot of the interaction frequencies $\nu_B^e(\rho)$ and $\nu_A^e(\rho)$. We remark that the results for the pressure, the lane changing probabilities and the collision frequencies have been slightly smoothed.

Finally, we plot in Figure (9) the leading vehicle distributions obtained in two ways.

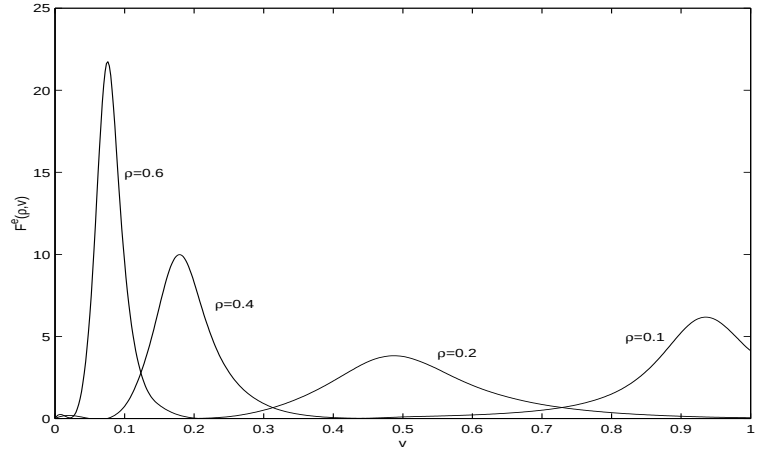

Figure 4: Kinetic distribution functions for $\rho = 0.1, 0.2, 0.4, 0.6$

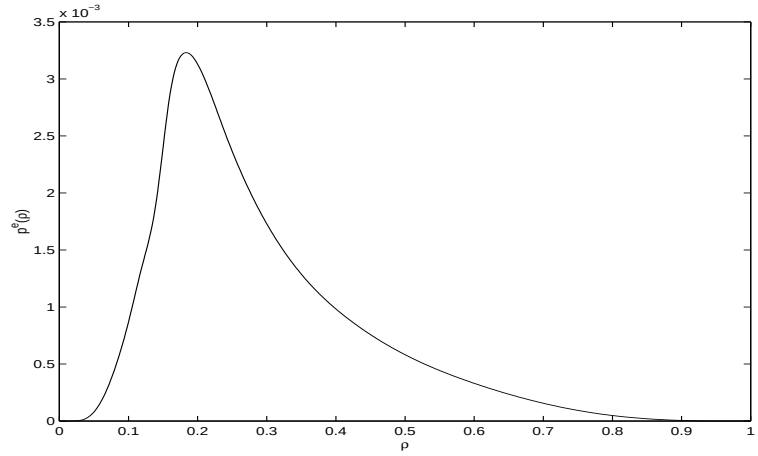

Figure 5: Traffic pressure $p_e(\rho)$

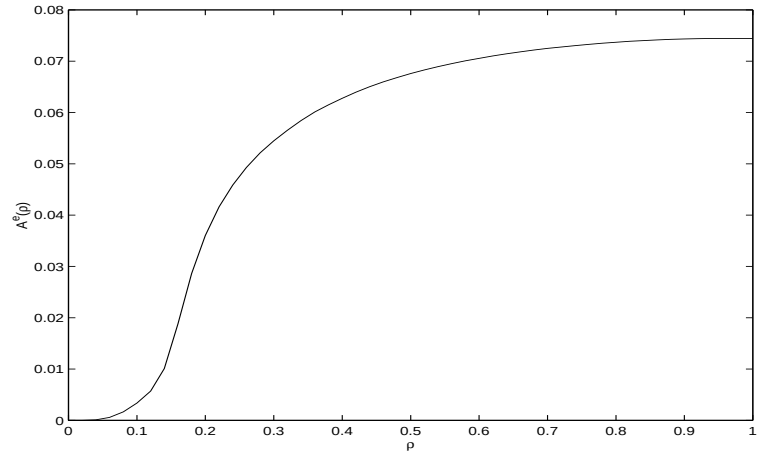

Figure 6: Enskog coefficient $A^e(\rho)$

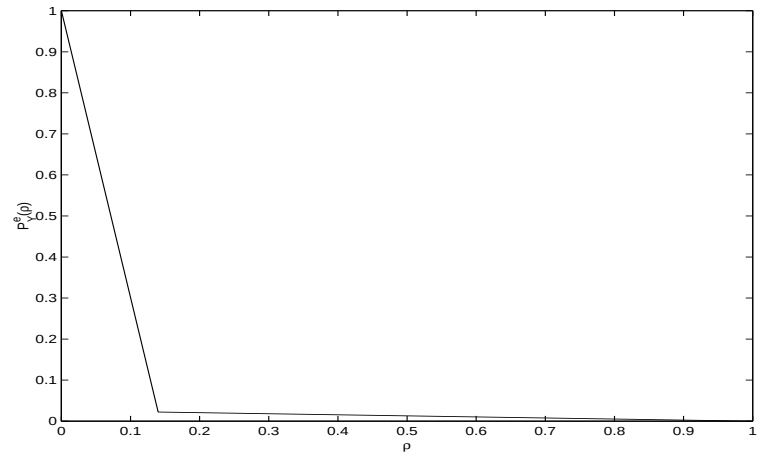

Figure 7: Lane changing probabilities $P_Y^e(\rho)$ due to interactions

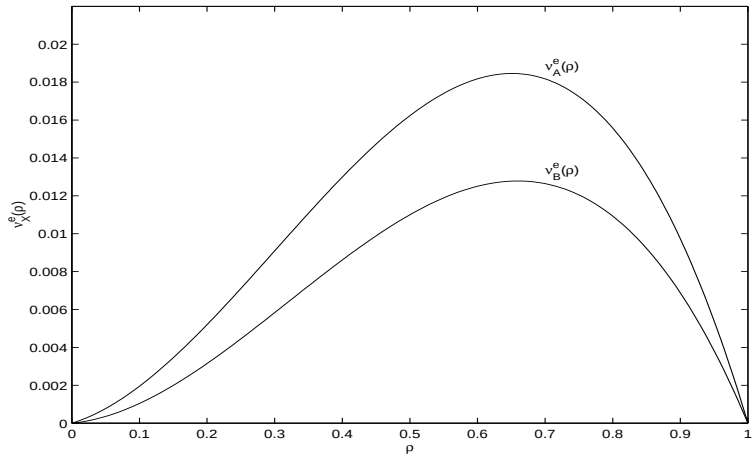

Figure 8: Interaction frequencies $\nu_B^e(\rho), \nu_A^e(\rho)$

We fix $\rho = 0.4$ and do not distinguish between vehicles with different velocities. First the microscopic model is used directly to obtain the distribution of the distances of the leading vehicle. This is compared to a distribution obtained by using the special form for q assumed in (2) or I,(6). $q(h; v, f)$ is computed using the distribution functions $f = f^e(\rho)$ obtained from the stationary distribution of the cumulative homogeneous kinetic equation. We plot again the velocity averaged version, i.e. we plot $< q(h; \cdot, f^e(\rho)) >$. One observes, that the leading vehicle distribution are nearly coincident for this value of ρ. For very small or very large values of ρ a slightly larger deviation is observed. This justifies the ad hoc choice of the leading vehicle distribution q for the kinetic model in I, Section 3.1., (6).

4 Inhomogeneous Simulations

In the following series of figures an inhomogeneous traffic flow situation is shown. We refer, e.g., to [2], for other simulations of macroscopic multilane models. We consider a highway with a reduction of the number of lanes from 3 to 2 after two thirds of the highway under consideration. The length L of the highway is equal to 1000. The lane drop is at the point $x = 600$.

The example is calculated with the multilane fluid dynamic equations stated in (19), (20) in I, Section 4.2. The coefficients are determined from the kinetic model and have been computed in the last section. Additionally, we increase the lane changing rates $\frac{1}{T_\alpha^L}$ and $\frac{1}{T_\alpha^R}$ defined in I, Section 4.2 by adding a fixed quantity independent of ρ in order to account for spontaneous lane changing not due to interactions with other cars. This has been neglected in the model so far. Looking at the values of $\nu_B^e(\rho)$ in Figure (8), we have chosen the value 0.005 as the additional lane changing

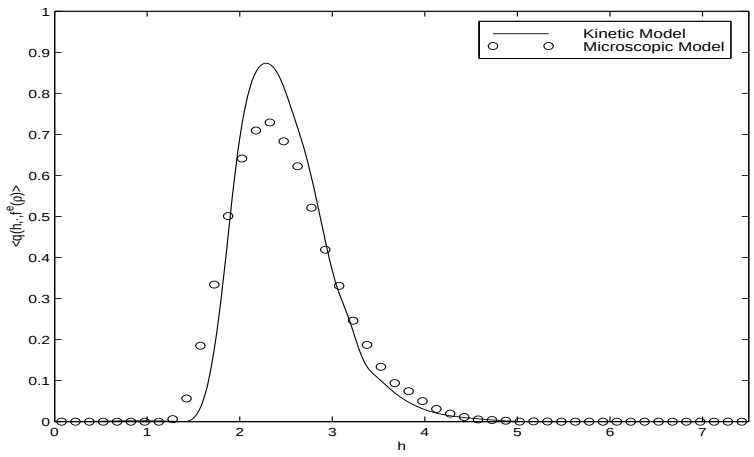

Figure 9: Leading vehicle distributions for $\rho = 0.4$

rate due to spontaneous lane changing. Here, obviously other models can be taken. For example, models, where the above lane changing rate is assumed to depend on ρ, may be used. We refer to [2] for different models and to [8] for experimental investigations. In front of the lane drop an additional strong increase of the lane changing frequency to the right is included on the left lane in order to obtain an empty highway on this lane just in front of the lane drop. (The size of this lane changing area is $\Delta x = 50$, the increase in lane changing frequency is $10\frac{w}{\Delta x}$.)

We start with an empty highway and prescribe the incoming values at 0. The number of ingoing vehicles is equal on all lanes. Moreover, a constant flux of incoming vehicles is used. The solutions of the macroscopic equation is shown in Figures (10) and (11) for all lanes and different times. The density ρ on the three lanes is plotted in Figure (10), the flux $q = \rho u$ in (11). Starting with an empty highway one observes in Figure (10) free flow of the vehicles until the stretch is completely filled with vehicles. The overall density is small compared to the maximal density, such that there is no influence of the lane drop. When the stretch finally is filled with vehicles, the density rises at the bottleneck. In particular, on the lane in the middle, to which the cars are changing from the right lane, one observes an increase in density. Later one observes the formation of a traffic jam, which is finally running backwards on all lanes. These results are, at least qualitatively, similiar to those that are observed in real traffic flow situations. A detailed comparison with measured data is left to future work. For a numerical simulation of a cumulative kinetic model and a comparison of the results with those of the associated macroscopic model, we refer to [5].

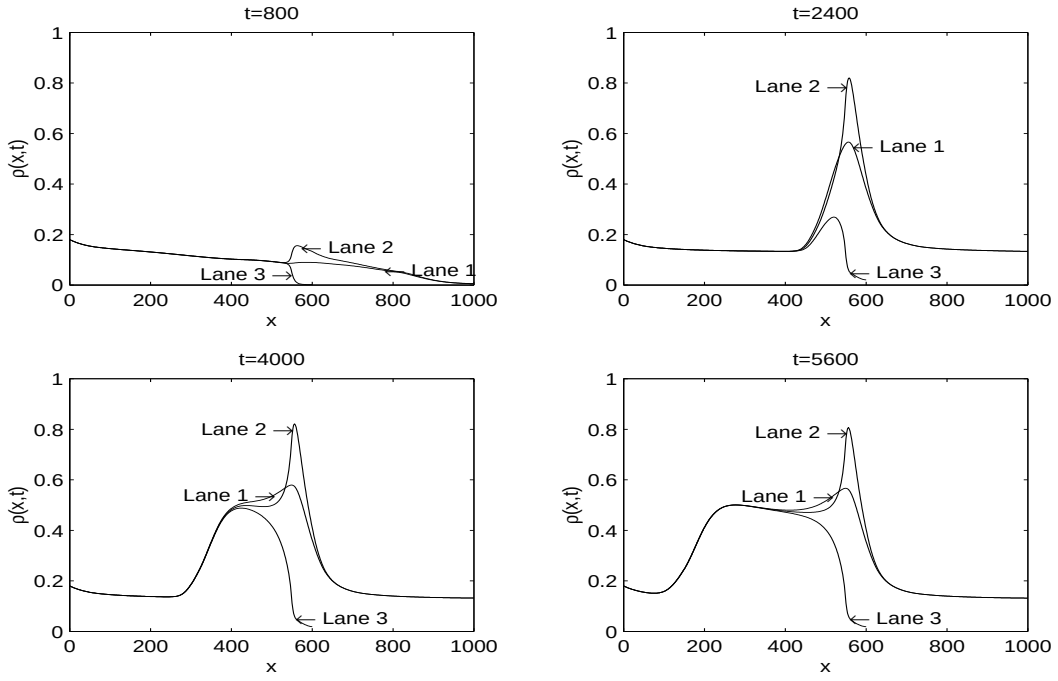

Figure 10: Time development of the density computed by the macroscopic multilane equations: Lane drop from 3 to 2 lanes at $x = 600$

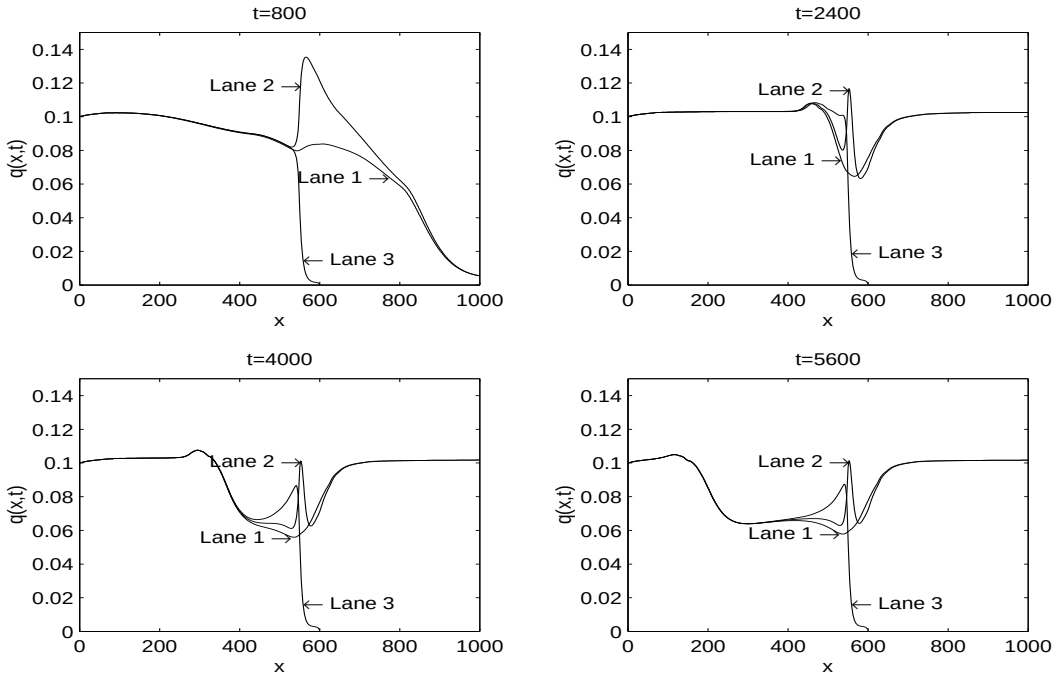

Figure 11: Time development of the flux computed by the macroscopic multilane equations: Lane drop from 3 to 2 lanes at $x = 600$

5 Stochastic correlation model

In this section the space homogeneous situation is treated in more detail using stochastic arguments. We introduce a basic stochastic model. A one lane highway with a large number of vehicles is considered. The distances between the vehicles are represented by probability variables $D_1, D_2, \cdots$. They are assumed to be independent. The location of the vehicles is given by the probability variables $X_1, X_2, \cdots$ defined by $X_{n+1} = X_n + D_n$ with X_1 given. The probability variables representing the velocities of the vehicles are denoted by $V_1, V_2, \cdots$. The velocities are distributed according to a given distribution function f with $\int_0^w f dv = \rho$. The stochastic process (V, X) can be viewed as a Markov renewal process, see [1].

In Part I, Section 3.1, the leading vehicle distribution, i.e. the distribution of the distances between the vehicles and their leading vehicles and the lane changing probabilities are used to obtain the kinetic model. The distribution of the distances $D_1, D_2, \cdots$ is discussed in the next subsection. An approximation for the lane changing probabilities is given in the second subsection.

5.1 Leading Vehicle Distribution

In this section the definition of the leading vehicle distribution is discussed. Each vehicle drives with an individual velocity v.

Looking at the microscopic model in I, Section 2 one observes that the braking line $H_B(v)$ represents the minimal distance between the vehicles. One part of the vehicles is assumed to be independent or freely driving. More exactly, they are assumed to have exponentially distributed leading vehicles, i.e. the density of the leading vehicle distribution for a vehicle with velocity v is

$$q(h; v, f) = \tilde{\lambda} e^{-\tilde{\lambda}(h - H_B(v))} \chi_{[H_B(v), \infty)}(h).$$

The parameter $\tilde{\lambda}$ is determined by the requirement that the mean space between the cars is equal to $\frac{1}{\rho}$ given by

$$< \int_0^\infty h q(h; v, f) dh >= \frac{1}{\rho}. \tag{1}$$

Looking again at the microscopic model one observes that most of the cars are trapped between braking and acceleration line. They are in a following behaviour oscillating between the braking and acceleration line. We assume therefore that only a part of the vehicles $((1 - \lambda), \lambda < 1)$ has exponentially distributed leading vehicles and the other part (λ) has a following behaviour. For this part we assume that the

headway is uniformly distributed between braking and acceleration line H_B and H_A. One obtains

$$\begin{aligned} q(h;v,f) &= (1-\lambda)\tilde{\rho}e^{-\tilde{\rho}(h-H_B(v))}\chi_{[H_B(v),\infty)}(h) \\ &+ \lambda\frac{1}{H_A(v)-H_B(v)}\chi_{[H_B(v),H_A(v)}(h) \end{aligned} \tag{2}$$

with the reduced density $\tilde{\rho}$ determined in such a way that (1) is fulfilled:

$$\tilde{\rho} = \frac{(1-\lambda)\rho}{1-\rho[(1-\lambda) < H_B > +\frac{\lambda}{2}(< H_B > + < H_A >)]}. \tag{3}$$

Here $(1-\lambda) < H_B > +\frac{\lambda}{2}(< H_B > + < H_A >)$ is the average space required per vehicle with exponentially distributed leading vehicles, if the rest is assumed to be distributed between H_B and H_A.

5.2 Lane Changing Probabilities

Determination of the probability of a gap is difficult for the general situation considered above. Moreover, this is not really the situation one has in mind. Instead one considers a homogeneous situation not depending on the special starting point X_1. Therefore, one determines an asymptotic distribution at infinity of the above process or, equivalently, one uses a so called stationary renewal process, see [3, 1].

The probability variables $D_i, i = 1, 2, \cdots$ are distributed according to the density $q(h; V_i, f)$. The velocity variables $V_i, i = 1, 2, \cdots$ are distributed according to f and independent of the D_i. We mention that the expectation of D_i is given by $E(D_i) = \mu = \frac{1}{\rho}$ according to the definition of q. In particular $E(D_i)$ is independent of i.

One looks at a fixed spatial point x and determines the distribution of the distance B_x between the point x and the next car behind x and the distance F_x between x and the next car in front of x:

$$\begin{aligned} B_x &= x - X_{N_x} \\ F_x &= X_{N_x+1} - x, \end{aligned}$$

if $X_{N_x} \leq x < X_{N_x+1}$. In the language of renewal processes B_x and F_x are the so called current and excess life. Obviously, $P(F_x \geq h_1, B_x \geq h_2)$ gives the probability for a gap of length h_1 in front of x and of length h_2 behind x. The asymptotic value of this probability as x tends to infinity is obtained using the renewal theorem, see e.g. [3, 1]. Rewriting the results obtained in [1] for the present context, one obtains:

$$P(F_x \geq h_1, B_x \geq h_2) = \frac{1}{\mu}\int_{h_1+h_2}^{\infty}[1- < Q(h;\cdot,f) >]dh$$

with the distribution function Q defined by

$$Q(h;v,f) = \int_0^h q(h';v,f)dh'. \tag{4}$$

This leads to

$$P(F_x \geq h_1, B_x \geq h_2) =< \rho \int_{h_1+h_2}^{\infty} \int_h^{\infty} q(h',\cdot,f)dh'dh > . \tag{5}$$

These considerations are now used to determine the lane changing probabilities $p_Y(v,v',f)$:

Due to the considerations in I, Section 3.1 the driver changes to the new lane, if the distance after the lane change between the changing car with velocity v and its leading car on the new lane is at least $H_Y^S(v), Y = L, R$. Moreover, the distance between the changing car and its follower on the new lane with velocity v' must be at least $H_Y^S(v'), Y = L, R$.

Setting $h_1 = H_Y^S(v)$ and $h_2 = H_Y^S(v')$ in the above formula leads therefore to the desired lane changing probability $p_Y(v,v',f)$ used in I, Section 3.1:

$$p_Y(v,v',f) =< \rho \int_{H_Y^S(v)+H_Y^S(v')}^{\infty} \int_h^{\infty} q(h',\cdot,f)dh'dh > . \tag{6}$$

Using the expression (2) for q a more explicit expression for $p_Y(v,v',f)$ is given by averaging the function $\tilde{p}_Y(v,v',\tilde{v},f)$ given below with respect to $\tilde{v}$:

$$p_Y(v,v',f) =< \tilde{p}_Y(v,v',\cdot,f) > .$$

$\tilde{p}_Y(v,v',f)$ is given by

$$p_Y(v,v',\tilde{v},f) = \rho R(H_Y^S(v) + H_Y^S(v'),\tilde{v},f)$$

with

$$R(h,v,f) = (1-\lambda)R_0(h,v,f) + \lambda R_1(h,v,f),$$

where

$$R_0(h,v,f) = \begin{cases} \frac{1}{\tilde{\rho}} + H_B(v) - h & \text{if } h < H_B(v) \\ \frac{1}{\tilde{\rho}} e^{-\tilde{\rho}(h-H_B(v))} & \text{if } H_A(v) > h > H_B(v) \\ \frac{1}{\tilde{\rho}} e^{-\tilde{\rho}(h-H_B(v))} & \text{if } H_A(v) < h \end{cases}$$

and

$$R_1(h,v,f) = \begin{cases} H_B(v) - h + \frac{H_A(v)-H_B(v)}{2} & \text{if } h < H_B(v) \\ \frac{(H_A(v)-h)^2}{2(H_A(v)-H_B(v))} & \text{if } H_A(v) > h > H_B(v) \\ 0 & \text{if } H_A(v) < h \end{cases} .$$

6 Conclusions

We have thus obtained a consistent new hierarchy of models ranging from a microscopic follow the leader model to a macroscopic fluid dynamic multilane model. In particular, a derivation procedure for kinetic and macroscopic traffic flow models is given. The basic features of this hierarchy are:

- The models are based on reaction thresholds with values derived from experimental data.
- The kinetic model uses a leading vehicle distribution derived from the behaviour on the microscopic level. This takes into account the strongly correlated behaviour of the vehicles.
- An Enskog like kinetic multilane model and a new cumulative model is derived. The cumulative model is derived from the multilane one.
- Macroscopic multilane models are derived by determining the coefficients from the stationary solution of the cumulative, homogeneous kinetic equation.
- The derivation of the macroscopic and kinetic equations is supported by numerical analysis. Numerical computations are presented on all levels and a comparison of the results on different levels is given.
- Further work is required for numerical simulations of the inhomogeneous kinetic multilane equations and a comparison of kinetic and macroscopic multilane results.

Acknowledgements
This work was supported by a grant under the program 'Wirtschaftsnahe Forschung' (Ministry of Economy, Rheinland Pfalz, Germany). In particular, we are grateful to B. Klar for pointing out some important stochastic details to us. Finally we wish to thank G. Gramlich and U. Fromknecht for help with parts of the numerical simulations.

References

[1] E. Cinlar. *Introduction to stochastic processes.* Prentice-Hall, 1975.

[2] D. Helbing and A. Greiner. Modeling and simulation of multi-lane traffic flow. *preprint, Univ. of Stuttgart.*

[3] S. Karlin and H.M. Taylor. *A first course in stochastic processes.* Academic Press, 1974.

[4] A. Klar, R.D. Kuehne, and R. Wegener. Mathematical models for vehicular traffic. *Surv. Math. Ind.*, 6:215, 1996.

[5] A. Klar and R. Wegener. Enskog-like kinetic models for vehicular traffic. *J. Stat. Phys.*, 87:91, 1997.

[6] A. Klar and R. Wegener. A hierachy of models for multilane vehicular traffic I: Modeling. *preprint*, 1997.

[7] R.D. Kühne and M.B. Rödiger. Macroscopic simulation model for freeway traffic with jams and stop-start waves. In B.L. Nelson, W.D. Kelton, and G.M. Clark, editors, *Proceedings of the 1991 Winter Simulation Conference*, page 762, 1991.

[8] U. Sparmann. *Spurwechselvorgaenge auf zweispurigen BAB-Richtungsfahrbahnen.* Bundesministerium fuer Verkehr,Abt. Strassenbau, Bonn-Bad Godesberg, Germany, 1978.